Available online at www.sciencedirect.com

ScienceDirect

Energy Procedia 4 (2011) 5170–5177

Energy Procedia

www.elsevier.com/locate/procedia

GHGT-10

Sealing rock characteristics under the influence of CO_2

Alexandra Amann[a], Margret Waschbüsch[a]1*, Pieter Bertier[b], Andreas Busch[c], Bernhard M. Krooss[a], Ralf Littke[a]

[a]*Institute of Geology and Geochemistry of Petroleum and Coal, RWTH Aachen University, Lochnerstr. 4-20, D-52056 Aachen, Germany*
[a]*Institute of Clay and Interface Mineralogy, RWTH Aachen University, Germany*
[c]*Shell International E&P, Kessler Park 1, NL-2288 GS Rijswijk, The Netherlands*

Abstract

To ensure the long-term safety of geological CO_2 storage sites, such as saline aquifers or depleted gas- and oilfields, the overburden must be able to effectively retain in place the CO_2 (either gaseous, supercritical or in dissolved state). In this study the caprock sealing efficiency and potential petrophysical and mineralogical changes of caprock integrity due to CO_2 exposure are being investigated. Analysis techniques include XRD for mineralogy and N_2-BET for specific surface determination, but also high-pressure CO_2 sorption and fluid flow experiments to study the sorption (retardation) and transport/capillary sealing characteristics of argillaceous caprocks.

As this study is of generic nature, argillaceous samples and one marl-/limestone have been selected from different locations, covering the scope from poorly consolidated clays to highly compacted shale/siltstones. The first results indicate that, except for the very heterogeneous marl-/limestone (water permeability values of approximately 10^{-18} m²), all samples have very good to excellent sealing properties. Absolute water permeability values are in the nDarcy (10^{-9} Darcy) to sub-nDarcy range ($k_{abs(water)} \leq 10^{-21}$ m²) and the capillary breakthrough experiments indicate that the clay-rich samples can retain the supercritical CO_2 phase up to capillary pressures of at least 10 MPa. Even though samples are acting as effective capillary seals up to 10 MPa, a very small CO_2 flux could be detected, which is interpreted to be due to CO_2 diffusion through the rock sample. Sorption measurements indicate the maximum CO_2 sorption capacity to vary between 0.25 and 0.63 mmol/g. This is significant and therefore sorption in thick argillaceous caprock layers may provide an important sink for CO_2 leaking from underlying storage reservoirs.

Keywords: CO_2 ; sealing efficiency ; caprocks ; shales ; fluid flow ; adsorption ;

1. Introduction

Clay-rich (argillaceous) formations with very low permeabilities and high capillary entry pressures are, besides salt or anhydrite, favorable caprock lithotypes above potential CO_2 storage reservoirs. Additionally, argillaceous rocks themselves may store a certain amount of CO_2 by sorption, which would slow down the process of

* Corresponding authors. Tel.: +49-241-80-95752; fax: +49-241-80-92152
E-mail address: waschbuesch@lek.rwth-aachen.de

doi:10.1016/j.egypro.2011.02.494

penetration/leakage [1]. However, depending on the sample mineralogy CO_2/fluid/rock interactions may lead to the dissolution and precipitation of minerals and result in structural changes of the pore system. In the best case these alterations may enhance the sealing capacity. In the worst case, CO_2/fluid/rock alteration may result in a reduction of capillary entry pressures and increase the risk of leakage [2].

In this study we aim to determine relevant parameters controlling the sealing efficiency of caprocks. Fluid transport and retardation properties are investigated in the laboratory under reservoir temperature and pressure conditions relevant for CO_2 storage. Measurements performed in this study enable us to provide estimates of the sealing capacity of argillaceous caprocks and to determine the potential of shales for adsorbing CO_2 and thus retarding gas leakage.

2. Samples

Rock samples were provided by several companies and institutions listed in Table 1. The cores were drilled in the context of CO_2 storage projects or research projects for nuclear waste deposition, which have similar requirements for the integrity of caprocks.

The mineral composition of all samples was determined by X-ray diffraction (XRD) on random powder preparations. The Rietveld refinement method was applied for quantification using the BGMN software (http://www.bgmn.de).

Table 1: List of companies and institutions and their provided caprock samples

Sample no.	Origin	Location	Type	Major compounds/minerals
CS_01 - CS_11	Shell International Exploration and Production	confidential	Compacted Silt/Shale, diagenetically rather mature shale	Quartz, feldspars, clays and minor amounts of siderite and pyrite; clay mineralogy is dominated by illite; smectite is present as a mixed-layer structure with illite
CS_20/21	Mont Terri Rock Laboratory	St. Ursanne, Switzerland	Opalinus Clay (weak mudstone - Jurassic)	Illite, smectite and kaolinite.
CS_22 - CS_27	ONDRAF/ NIRAS SCK-CEN	Mol, Belgium, HADES project	Boom Clay (homogeneous clay - Tertiary)	
CS_12 - CS_16	Holcim AG	Höver (open pit quarry), Hannover, Germany	Marl-/Limestone (Lower Campanian)	Very heterogeneous with respect to its clay content; some parts are purely limestone, some parts contain some minor amounts of clay
CS_43/44	CO_2SINK project	Ketzin, Germany	Anhydritic clay-rich mudrocks (Weser formation)	Very fine-grained red shale/claystone with greenish, bleached nodules. Clay content of about 65 %, mostly well-ordered illite-smectite (R3), minor chlorite and kaolinite, low quartz content (< 10%), feldspar content < 10%, mostly albite, carbonate content about 15 %, mostly ankerite, traces of calcite and siderite. Minor amounts of hematite, halite and anhydrite/gypsum

The samples were first characterized with respect to their petrophysical properties. The results obtained so far are listed in Table 2. The porosity was measured by mercury injection porosimetry using a Micromeritics AutoPore III 9400 porosimeter. Grain density was derived from either mercury porosimetry or gas expansion (pycnometry) during sorption measurements (see below). The total organic carbon (TOC) and the total inorganic carbon (TIC) contents were measured with a LECO RC-412 Multiphase Carbon/Hydrogen/Moisture Determinator. The specific N_2-BET surface area was determined from low-pressure sorption isotherms measured in an AUTOSORB-1 volumetric gas sorption analyzer (Quantachrome Corporation).

Table 2: Petrophysical properties of samples analyzed in this study, (TOC: Total organic carbon, TIC: Total inorganic carbon, n. a.: not yet analyzed)

Samples	Sample no.	Phi from Hg-porosi-metry	Grain density from Hg-porosimetry (g/cm^3)	TOC (weight%)	TIC (weight%)	Particle size for BET (µm)	N_2-BET before sorption (m^2/g)
Mudstone samples (Shell)	CS_01	n. a.	n. a.	2.45	0.2	200-500	7.7
	CS_02	n. a.	n. a.	3.7	0.6	200-500	11.0
	CS_03	7.3	2.3	2.1	0.1	200-500	10.0
Marl	CS_12	15.9	2.3	n. a.	n. a.	200-500	40.0
Opalinus Clay	CS_20	n. a.	n. a.	n. a.	n. a.	< 200	n. a.
Boom Clay	CS_27	26.7	2.3	n. a.	n. a.	500-1000	n. a.
Dolomitic mudrocks from the Ketzin site	CS_43	12.3	2.4	n. a.	n. a.	500-1000	n. a.
	CS_44	n. a.	n. a.	n. a.	n. a.	500-1000	n. a.

3. Sample preparation

3.1. Preparation for the sorption experiments

For the sorption experiments powdered samples were used to minimize the equilibration time and reduce the duration of experiments. Systematic measurements were performed to select suitable particle size fractions for well-defined experimental conditions and to ensure, that the crushing of the sample did not destroy the mineralogical texture. Different particle size fractions were sieved and analyzed to ensure that the selected fractions were representative for the bulk rock. Based on these analyses, fractions between 125 and 1000 µm were used for the sorption tests.

The moisture content of the samples influences the sorption capacity significantly. On the one hand, the CO_2 uptake increases by dissolution of CO_2 in the water, on the other hand, a competitive adsorption between the water molecules and the CO_2 decreases the sorption capacity [3]. In the first series of sorption measurements dry samples were used to eliminate the effect of moisture. The samples were dried at 105 °C or 200 °C for 24 h under vacuum. Further measurements are planned to study CO_2 sorption on moisture-equilibrated samples.

3.2. Preparation for the fluid flow measurements

Fluid flow measurements require plane-parallel sample plugs. These plugs were drilled with diameters of either 28.5 or 38 mm. To reduce the risk of disintegration, samples were fixed in axial direction during the drilling process and compressed air was used as cooling agent. The thickness of the plugs ranges between 10 and 30 mm. Some samples contained micro fissures/fractures and could not be drilled successfully (clays from Mont Terri and from Bure).

4. Excess adsorption experiments

4.1. Manometric method

High-pressure gas sorption isotherms were determined using a manometric set-up (Figure 2). Gas pressures up to 25 MPa and maximum temperatures of 75 °C can be achieved with this set-up. It consists of a stainless-steel cell including the sample, a temperature sensor (Pt 100), a reference cell to determine the gas inlet into the sample cell and a high-precision pressure transducer. The gas supply with He and CO_2 and the connection to the vacuum pump is controlled by a set of pneumatically operated valves. Helium, as a non-sorbing gas, is used for the volume calibration. The cells are located in a thermostatic oven to assure a constant temperature during the measurement. A detailed description of the method is given by [4], [5] and [6].

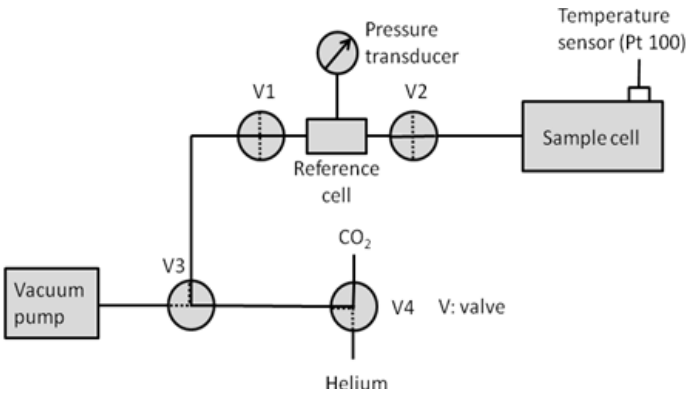

Figure 1: Manometric set-up for the CO2 excess sorption isotherm measurements

4.2. Results of the excess sorption experiments

The recorded pressures, temperature and volumes were evaluated in terms of excess (Gibbs) sorption capacity using an equation of state for CO_2 by Span and Wagner [7]. The CO_2 excess sorption isotherm usually shows a decrease at pressures above 8 MPa (see Figure 2). This coincides with and is due to the strong increase in CO_2 density at pressures between 8 to 12 MPa, when the density of the free CO_2 in the gas phase approaches the density of the adsorbed CO_2.

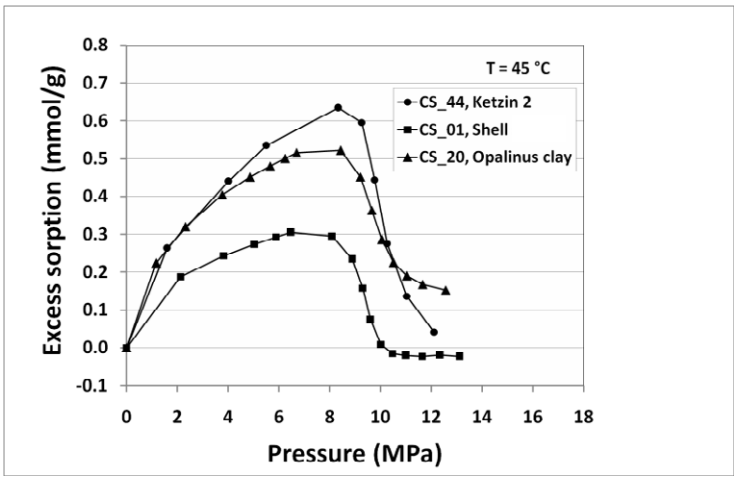

Figure 2: Excess sorption of CO_2 on Ketzin mudrocks, Shell mudstone and Opalinus clay at 45 °C (dry samples)

The excess adsorption isotherms of the caprock samples were measured at a temperature of 45 °C, which corresponds to a depth of about 1000 m. The curves show similar shapes besides their maximum sorption capacities vary between 0.25 mmol/g (CS_03) and 0.63 mmol/g (CS_44). Figure 2 only shows a selection of the recorded isotherms; a summary of results for all measured samples is provided in Table 1. Since data sets are not yet complete, no correlation study of sorption capacity with rock specific parameters like total organic carbon (TOC) content, mineralogy or specific surface area has been made.

Table 3: Maximum sorption capacity at 45 °C of dried samples

Samples	Sample no.	Particle size (µm)	Max. CO_2-sorption capacity (mmol/g)
Mudstone samples (Shell)	CS_01	125-200	0.31
	CS_01	200-500	0.28
	CS_02	200-500	0.35
	CS_03	200-500	0.25
Marl	CS_12	200-500	0.35
Opalinus Clay	CS_20	< 200	0.50
Boom Clay	CS_27	500-1000	0.56
Mudrocks from the Ketzin site	CS_43	500-1000	0.49
	CS_44	500-1000	0.63

5. Fluid flow measurements

5.1. Fluid flow cell

The fluid flow measurements are performed in triaxial flow cells, which allow measurements under controlled stress and temperature conditions [2], [8] and [10]. Cylindrical sample plugs of 28.5 or 38 mm diameter and a maximum length of 30 mm are used. The stainless-steel pistons are equipped with boreholes for fluid introduction and removal. The outer surface of the sample/piston arrangement is sealed with a double-layered sleeve of lead (Pb) foil (0.15 mm thickness) and either copper (Cu) or aluminium (Al) tubes. At first, application of a high confining pressure of at least 30 MPa for approximately one hour ensures a leak-tight seal around the sample plugs. The leak-tightness of this double-layered sleeve system has been tested extensively in gas diffusion experiments [8]. The pressures are then set to the required in-situ conditions. The same arrangement was used for single-phase permeability measurements and gas breakthrough experiments.

For poorly compacted/weak mudstones, like the Opalinus or the Boom Clay, the high initial pressurization might lead to additional artificial compaction and concomitant reduction of porosity and permeability. Recently, mineralogical analysis after the CO_2 experiments revealed, that the lead foil reacts with CO_2 to form cerussite, a Pb-carbonate. Therefore, alternative sealing methods are presently being tested.

5.2. Experimental Procedures

The standard experimental procedure starts with a water/brine saturation experiment yielding absolute or intrinsic permeability coefficients. Permeability coefficients (k_{abs}) are calculated according to Darcy's law for incompressible fluids:

$$k_{abs} = -\frac{Q \cdot \eta}{A} \frac{\Delta x}{\Delta P}$$

Here Q [m³/s] is the volume flux, η [Pa·s] is the dynamic viscosity of the permeating fluid, $\Delta P/\Delta x$ [Pa/m] is the

fluid pressure gradient and A [m²] the sample cross-section area. Complete water-saturation of the conducting pore system is assumed when single-phase flow is constant for an extended period of time.

Prior to the breakthrough experiment a leak test is performed. Both compartments are pressurized with helium in order to check the system for potential leaks. The assessment of leakage rates in combination with a careful volume calibration allows an accurate mass balance of the system (e. g. gas transport from the reservoirs into the sample plug). Assuming that the pressure drop within the first hours of the leak test is purely due to the uptake of gas by the sample (leak-free system), we can estimate the effective diffusion coefficient according to the approach described by Crank [9] for diffusion of solute (gas) from a "well-stirred solution" into an infinite plane sheet (sample plug). The boundary conditions correspond to our experimental set-up: Initially ($t = 0$) the plug is free of gas and the gas concentration within the reservoir ("well-stirred solution") is at a maximum. At $t > 0$ the gas diffuses from the reservoir into the plug according to the chemical potential gradient (pressure gradient) across the reservoir/sample boundary.

After the leak tests the gas breakthrough experiment is started by imposing a gas pressure difference across the rock samples. The resulting gas flux is monitored as a function of time by means of pressure changes in a closed downstream reservoir of known volume. Both, the drainage and imbibition path can be monitored. Drainage experiments, i.e. the step-wise increase of pressure difference until gas breakthrough, yield information on the drainage capillary breakthrough pressure. The imbibition method [10] provides information on the capillary snap-off pressure, where gas flow stops. In general, the drainage breakthrough pressure is higher than the imbibition snap-off pressure.

During the first period of the gas breakthrough experiment residual water is displaced from the reservoir across the sample plug before the gas phase reaches the sample surface. At this stage, capillary forces are not acting and the recorded pressure decay curve can be used to calculate the absolute water permeability [2].

5.3. Experimental results

Fluid flow measurements on extremely tight rocks are challenging. Experience shows that sample preparation constitutes a major difficulty and has to be adapted individually for each type of sample material. Samples that are not adequately treated tend to lose much of their in-situ moisture and disintegrate during preparation. Long-term experiments taking up to several months carry an additional risk of sample or seal failure due to corrosion or deformation processes.

Up to present, 7 samples were successfully drilled and installed into fluid flow cells. The results are listed in Table 4. Among these samples two types of materials were identified: those with very high sealing efficiency (CS_01-05) and those with low retention capacity (CS_12).

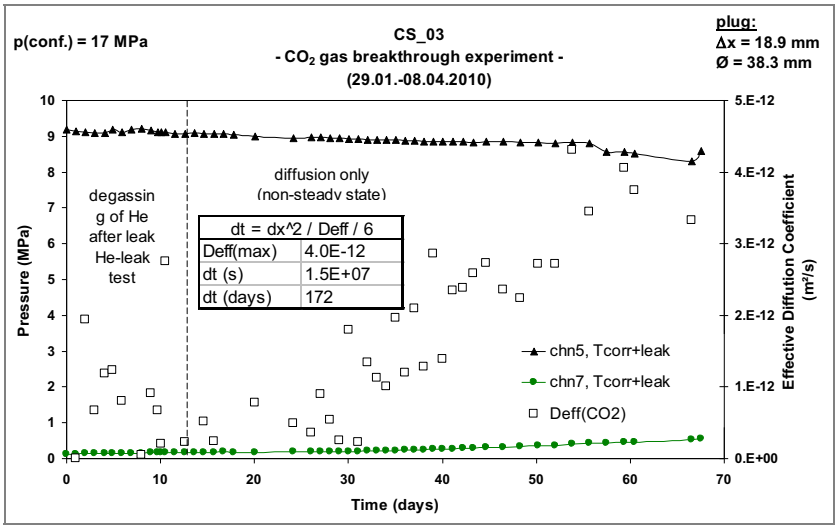

Figure 3: CO_2 gas breakthrough experiment on sample CS_03

Samples CS_01-03 and CS_05 are characterized by extremely low absolute permeability coefficients in the sub-nDarcy range ($<10^{-21}$ m²). Serial gas breakthrough experiments revealed that capillary displacement of water did not occur for He pressures up to 20 MPa (CS_01) and CO_2 pressures up to 9 MPa (CS_03).

Here, only diffusive transport of gas occurred. Effective diffusion coefficients for He derived from the experimental data range from $2 \cdot 10^{-10}$ to $6 \cdot 10^{-10}$ m²/s. The effective CO_2 diffusion coefficients estimated from the pressure increase on the downstream side increased with time (Figure 3). This indicates that steady state conditions have not been reached during the test. A simple calculation of the time lag ($\Delta t = (6 \cdot \Delta x^2)/D_{eff}$; [9] p.51) reveals that a period of 170 days would be required to establish nearly steady state conditions. Sorption or other CO_2/fluid/rock interactions would lead to an additional delay. Therefore the "maximum CO_2 diffusion coefficients" in Table 4 should be taken as lower limits. The experiments show that at the low transport rate levels prevailing here, viscous (Darcy) flow, diffusion and sorptive uptake processes can no longer be clearly discriminated.

Table 4: Results from fluid flow experiments; k_{gas}(dry) = single-phase gas permeability on as-received or dry sample; k_{abs}(water) = single-phase water permeability determined from saturation experiments; $k_{abs\text{-}water}$(gbthr.) = absolute permeability determined from gas breakthrough experiments (gbthr.); D_{eff} = effective diffusion coefficient taken from pressure decay during leak test or from the pressure increase on the low pressure side during gas breakthrough experiments; $P_{(brthr)}$ = drainage breakthrough pressure; $p_{(snap\text{-}off)}$ = imbibition snap-off pressure

Sample no.	Kgas (dry) m²	k_{abs} (water perm.) m²	D_{eff} (leak test) m²/s	D_{eff} (gbthr.) m²/s	$K_{abs\text{-}water}$ (gbthr.) m²	$P_{(brthr)}$ & $p_{(snap\text{-}off)}$, MPa	Experimental conditions
CS_01		**(7.2±0.5)*10^{-22}**	**2.2*10^{-10} (He)**	**3*10^{-10} (He)**	**~ 1*10^{-22}**	**-**	**P(conf.) = 37 MPa T =20-25 °C Max. p(He) = 20 MPa**
				→ He gas breakthrough: mass balance inconsistent!			
CS_02		**(8.6±0.3)*10^{-22}**	**6*10^{-10} (He)**	**2*10^{-10} (He) 8*10^{-11} (CO_2, max value in step III)**	**3*10^{-22} 1.3*10^{-22}**	**-**	**P(conf.) = 20-21 MPa T =30-42 °C Max. p(He) = 10 MPa Max. p(CO_2) = 7 MPa**
				→ He gas breakthrough: mass balance inconsistent! → CO_2 gas breakthrough: mass balance o.k.; increasing diffusion coefficients			**New flow cell with additional Pb and Al-foil**
CS_03		(2.7±0.1)*10^{-22}	nd	4*10^{-12} (CO_2, max)		-	**P(conf.) = 15 MPa T =38 °C Max. p(CO_2) = 9 MPa**
CS_04		(1.5±0.07)*10^{-21}	Sample broke during initial loading. Further experiments were not performed.				
CS_05		(9.3±0.6)*10^{-23}					**P(conf.) = 15 MPa T =20-35 °C**
CS_12 #1		9*10^{-19}	New cell: system not diffusion tight !! Limited evaluation		**9*10^{-19}**	**(1.3-1.9, snap-off overestimated)**	**P(conf.) = 22 MPa T =25 °C**
CS_12 #2	2*10^{-17}	3*10^{-18} 2.5*10^{-18} (after gbthr)	9*10^{-10} (He)	-	4.4*10^{-18}	1.25-1.32 (bthr) 0.63 (snap-off)	P(conf.) = 22 MPa T =24-45 °C

Sample CS_04 exhibited a slightly higher permeability ($1.5 \pm 0.07 \cdot 10^{-21}$ m²) than the other samples from this sequence. It was damaged at the beginning of the test due to accidental application of excessive axial load without appropriate confining pressure. After the test a fracture running through the sample was observed. As this sample had been stressed too much in the beginning it was decided to discontinue the measurements.

For sample CS_12, which had a higher permeability ($k_{abs} = 10^{-18}$-10^{-19} m²) a series of alternating gas breakthrough tests with He and CO_2 was planned. Repeated He gas breakthrough experiments on the second plug yielded the following key parameters and conclusions: (a) the absolute water permeability before and after He gas breakthrough experiments is reproducible (k_{abs}(water) = 2.5-3·10^{-18} m²), (b) absolute water permeability coefficients

derived from the gas breakthrough experiment are higher than from steady-state experiments ($4.4 \cdot 10^{-18}$ m²), (c) the snap-off pressure is approximately half of the drainage breakthrough pressure (0.63 vs. 1.25 MPa), and (d) the snap-off pressure is reproducible.

6. Summary and conclusion

In this study clay-rich lithotypes of different mineral compositions and compaction states are being investigated. Samples are characterized with respect to their sealing efficiency by means of their tightness (viscous flow, diffusion) and retention (sorption) properties.

So far, nine high-pressure CO_2 sorption measurements were performed on dried samples (T = 45°C, pressure up to 14 MPa). The maximum excess sorption capacities range from 0.2 - 0.6 mmol/g. No dependence of sorption capacity on the N_2-BET specific surface or on the carbon content was observed.

The first samples investigated are characterized by very good sealing properties (CS_01-CS_05). Absolute water permeability values are in the nDarcy to sub-nDarcy range and capillary breakthrough experiments indicate that the samples retain the supercritical CO_2 phase up to capillary pressures of at least 9 MPa. Even though samples are acting as effective capillary seals up to 9 MPa, a very small CO_2 flux could be detected, which is interpreted to be due to diffusion through the rock sample. Another sample (CS_12) proved to have a slightly lesser sealing efficiency. Permeabilities are in the order of 10^{-18} to 10^{-19} m², drainage capillary breakthrough pressure is 1.25 MPa and the imbibition snap-off pressure is 0.65 MPa.

7. Acknowledgements

The presented work is part of the CO_2Seals project, which is running from August 2008 to July 2011. It is incorporated into the GEOTECHNOLOGIEN R&D program funded by the German Federal Ministry of Education and Research (BMBF). CO2Seals is co-funded and accompanied scientifically by the industry partner Shell International Exploration and Production, Netherlands. Funding no.: 03G0681A

We would also like to thank the companies and institutions listed in Table 1 for providing the caprock samples.

8. References

[1] Busch A, Alles S, Gensterblum Y, Prinz D, Dewhurst DN, Raven MD, Stanjek H, Krooss BM. Carbon dioxide storage potential of shales. Int J Greenhouse Gas Control 2006; 2:297-308.

[2] Wollenweber J, Alles A, Busch A, Krooss BM, Stanjek H, Littke R. Experimental investigation of the CO_2 sealing efficiency of caprocks. Int. J. Greenhouse Gas Control 2010, 4.

[3] Kempka T, Waschbüsch M, Fernandez-Steeger TM, Azzam R. Sorptive storage of CO_2 on coal dust and flotation waste from coal processing in abandoned coal mines 2006. In: van Cotthem A, Charlier, R. ; Thimus, J.F. ; Tshibangu, J.P. (ed.): EUROCK 2006 - Multiphysics Coupling and Long Term Behaviour in Rock Mechanics, 9-11 May 2006, Liège (Belgium), p. 69-74.

[4] Krooss BM, van Bergen F, Gensterblum Y, Siemons N, Pagnier, HJM, David P. High-pressure methane and carbon dioxide adsorption on dry and moisture-equilibrated Pennsylvanian coals. Int. J. Coal Geol. 2002; 51:69–92.

[5] Busch A, Gensterblum Y, Krooss BM. Methane and CO_2 sorption and desorption measurements on dry Argonne Premium Coals: pure components and mixtures. Int. J. Coal Geol. 2003; 55:205–24.

[6] Siemons N, Busch A. Measurement and interpretation of supercritical CO_2 adsorption on worldwide coals. Int. J. Coal Geol. 2007; 69:229–42.

[7] Span R, Wagner W. A new equation of state for carbon dioxide covering the fluid region from the triple-point temperature to 1100 K at pressures up to 800 MPa. Journal of Physical and Chemical Reference Data 1996; 25 (6):1509– 96.

[8] Schlömer, S. and B. M. Krooss (1997). "Experimental characterisation of the hydrocarbon sealing efficiency of cap rocks." Marine and Petroleum Geology 14(5): 565-580.

[9] Crank, J. (1975). The Mathematics of Diffusion. Oxford, Clarendon Press.

[10] Hildenbrand A, Schlömer S, Krooss BM (2002) Gas breakthrough experiments on fine-grained sedimentary rocks." Geofluids 2: 3-23.